Annuaire de l'Universite de Sofia "St. Kliment Ohridski", Faculte de Physique, v. 103, 2010

THE DISPERSION AND COMPONENTS OF THE DOMINANT MODE ON THE IMAGE GUIDE FOR MILLIMETER WAVES

ILIYANA ARESTOVA, ROSITZA TOMOVA, GERGINA ANGELOVA

Department of Radiophysics and Electronics
Faculty of Physics, St. Kliment Ohridski University of Sofia, Bulgaria

Илияна Арестова, Росица Томова, Гергина Ангелова. ДИСПЕРСИЯ И КОМПОНЕНТИ НА ОСНОВНИЯ МОД В ОГЛЕДАЛЕН ДИЕЛЕКТРИЧЕН ВЪЛНОВОД ЗА МИЛИМЕТРОВИ ВЪЛНИ

Огледалният диелектричен вълновод е предавателна структура, която е изследвана интезивно с оглед на приложението й в милиметровия диапазон на електромагнитния спектър. Тя се счита за перспективна не само като предавателна структура, но и като база за изграждане на различни компоненти – насочени отклонители, изолатори и др. Тук е изследвана експериментално по метода на проходния резонатор (МПР) и числено по метода на крайните елементи (МКЕ) дисперсията на основния мод в огледален вълновод от поликор в честотния диапазон 28–38 GHz. Също така получено е разпределението на компонентите на основния мод чрез симулация по МКЕ и с помощта на електрични сонди.

Iliyana Arestova, Rositza Tomova, Gergina Angelova. THE DISPERSION AND COMPONENTS OF THE DOMINANT MODE ON THE IMAGE GUIDE FOR MILLIMETER WAVES

The image guide is a guiding structure which has been intensively investigated for application in the millimeter wavelength range. It has been considered as a perspective both for a guiding structure and for a possible base for design of components – directional couplers, isolators etc. Here we have studied experimentally by the cavity resonator method (CRM) and numerically by the finite element method (FEM) the dispersion on the alumina image guide in the frequency range of 28 – 38 GHz. Also, we have simulated by the FEM the distributions of the components of the dominant mode, and measured with the help of electric probes the electric field components.

***Keywords*:** dielectric waveguides, image guide, millimeter waves
***PACS number*:** 84.40.Az

For contact: Iliyana Arestova, St. Kliment Ohridski University of Sofia, Faculty of Physics, 5 James Bourchier blvd., Sofia 1164, phone 359 2 8161 724, e-mail: ilar@phys.uni-sofia.bg.

1. INTRODUCTION

The image guide (IG) is one of the possible solutions for design of components at millimeter wavelengths, particularly nonreciprocal components such as isolators and circulators [1, 2]. The configurations proposed [3-5] usually consist of a dielectric image guide coupled to the ferrite image guide. The coupled image guide structures (CIGSs) that have a different magnetization of the ferrite have been investigated – the longitudinal, transverse and mixed one. The first step in the design procedure of such complicated components on the base of the CIGSs seems to be the study of the dispersion characteristic and the components of the dominant mode of the IG.

The modes in the IG are hybrid – all of their components are not equal to zero. The rectangular geometry of the IG is preferred by the designers because of the simplicity to fabricate and the applicability at millimeter wave integrated circuits. On the other hand, the rectangular geometry of the IG does not permit to solve analytically the problem of the electromagnetic wave propagation. The classification of the modes on the IG that is usually used in the literature is given by Marcatili for the dielectric rectangular waveguide in the integrated optics [6]. According to this classification based on the Marcatilli's approximate method there are two families of modes – E^{y}_{mn} and E^{x}_{mn}. The upper index (x or y) stays for the so-called main (principal) component of the transverse electric field – E_x or E_y. The sub indexes m and n indicate the number of maxima the main component has within the dielectric core. The main transverse field components of the E^{y}_{mn} modes are E_y and H_x, and those for the E^{x}_{mn} modes – E_x and H_y. The dominant (fundamental) mode is E^{y}_{11} and the first and second higher order modes are E^{y}_{21} and E^{x}_{11}, which are degenerate according to Marcatili's consideration.

Some investigators after Marcatili have shown the shortcomings of his method and classification especially at microwave frequencies. More correct classification has been proposed in [7] after the exact calculation of the field distribution and phase constant done by the mode matching technique. The designation of the possible modes on the IG is based on the modes of a simple dielectric slab guide, where the E (TM) modes have only E_z, E_y and H_x components, and the H (TE) modes – only H_z, H_y and E_x components. The modes on the IG are designated as EH_{mn} and HE_{mn} – the mode is of an EH type if the E_z, E_y and H_x components are superior to the H_z, H_y and E_x, and of a HE type – if the contrary is true. Indices m and n show the number of maxima of the E_y component in the dielectric core along the Ox and Oy, respectively. According to this consideration the dominant mode in the IG ($\varepsilon_r = 12$) is EH_{11}, that is the E^{y}_{11} mode after Marcatili. The first higher order mode is HE_{11}, and the second – EH_{21}, the former corresponding to the E^{x}_{11} mode in Marcatilli's classification and the latter – to the E^{y}_{21}. These two modes are not degenerate and which of them is the first higher order mode depends on the dielectric constant and the aspect ratio of the dielectric core (the aspect ratio is equal to the width divided by the height of the dielectric core).

The detailed consideration of the bandwidth of a single mode operation of the IG is proposed in [8]. The upper frequency limit is equal to the cutoff frequency of the first higher order mode. The lower frequency limit could be defined from three different points of view involving the dispersion, wave-guiding properties and variation of the characteristic impedance. From the point of dispersion, the lower frequency limit is chosen to be the frequency, at which the phase velocity has changed by 20% from its value at the cutoff frequency of the first higher order mode. The lower frequency limit from the wave-guiding point of view is equal to that frequency at which the power ratio between air and dielectric becomes equals to unity. The third definition proposed has been based on the variation of the characteristic impedance – the lower frequency limit is equal to that frequency at which the characteristic impedance differs by 50% from the characteristic impedance at the cutoff frequency of the first higher order mode.

Here we have dealt with both experimental and numerical investigation of the alumina ($\varepsilon_r = 9.6$, $tg\delta_\varepsilon = 10^{-4}$) IG with a cross section of a x b = 2 x 0.97 mm^2 in the frequency range of 28 – 38 GHz. First, we have measured the dispersion characteristic by the cavity resonator method (CRM). After that, we have measured by using the movable electric probes the distribution of the electric field components of the dominant mode. The measured dispersion characteristics and distributions of the electric field components have been complemented with those obtained by the finite element method (FEM) simulation with the help of the 3D electromagnetic simulator.

2. EXPERIMENT

2.1. Experimental Setup

The experimental setup used in this investigation is shown in Fig.1a. The scalar network analyzer *1* works in the K_a band (26 – 38 GHz) and includes standard metal rectangular waveguide (SMRW) components with a cross section of 7.2 x 3.4 mm^2. The generator *2* can operate both in a swept and in a fixed frequency mode. The directional couplers *4* combined with the build-in detectors *5* permit a separation of the incident and the transmitted wave to and out of the structure under investigation *6*.

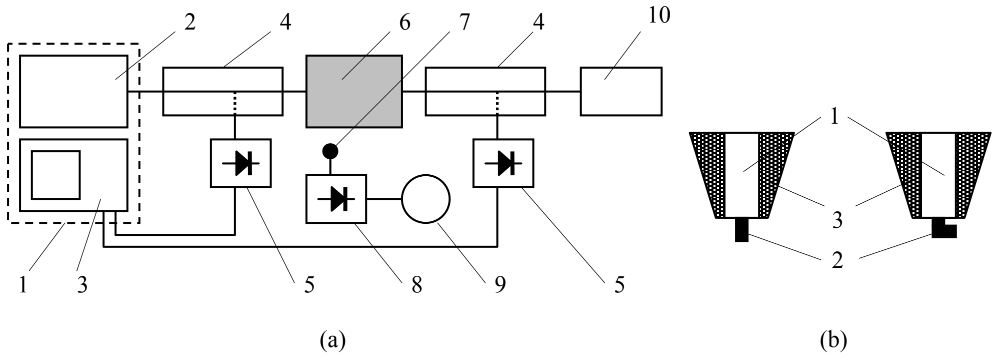

Fig. 1. The experimental setup (a) and the electric probes (b):
(a) 1 – scalar network analyzer; 2 – generator; 3 – indicator; 4 – directional couplers; 5 – build-in detectors; 6 – the structure under investigation; 7 – electric probe; 8 – waveguide detector; 9 – microvoltmeter; 10 – matched load;
(b) 1 – semi-rigid coaxial cable; 2 – inner conductor; 3 – absorbing coating

The configuration of the electric probes *7* used for the electric field sampling is shown in Fig.1b. We have used two different probes – the probe shown in the left has been used for the E_y component, and the one shown in the right – for both E_x and E_z components at the proper orientation. The electric probe for the E_y component contains a straight vertical section of the inner conductor, while the electric probe for E_x and E_z – a 90º bend section. Both electric probes represent a section of a semi-rigid coaxial cable (50 **Ω**, outer diameter 2.20 mm), which has its outer conductor removed at both ends on the length of about a quarter of a wavelength. One of the ends of the coaxial cable has been inserted into a hole in the middle of the broad wall of a SMRW section. One of the ports of the SMRW section has been shorted at about a quarter of a wavelength, and the second port has been connected with a waveguide detector *8*. The output of the detector has been connected to the DC microvoltmeter *9*, which is used as an indicator.

The electric probe has been mounted on a three axes mechanism [9], which has been made by a conjunction of a standard slotted line vernier mechanism and two micrometer coordinate tables. The vernier mechanism has been used for the positioning of the probe along the longitudinal axis *Oz* and permits an accuracy of 0.05 mm. The coordinate tables have been used for the positioning of the probe along the transverse axes *Ox* and *Oy* and give an accuracy of 0.01 mm.

The finite dimensions of the electric probes – a diameter of 0.51 mm and a length of about 2 mm, determine the accuracy of the electric field sampling. The diameter of the probe is much lesser than the guide wavelength and may not be taken into account. The length of the probes is only few times lesser than the guide wavelength and that's why the positioning of the probe at a given coordinate always implies the averaging of the electric field component along the respective axis. In particular, the electric probe for the E_y component averages the electric field along the height above the dielectric core. The electric probes for the E_x and E_z components perform the averaging along the *Ox* and *Oz* axes, respectively.

It is worth noting that the electric probe for the E_x and E_z component inevitably contains a small vertical section of the inner conductor due to its 90º bending, so it does register in some extent the E_y component as well. That makes this probe less perfect in comparison to the electric probe for the E_y component. When the E_x or E_z component in the structure under investigation is much lesser than the E_y component, the probe for the E_x and E_z component practically measures the E_y component. As we have noted earlier [10], the electric probe for the E_x and E_z component works appropriately when these components are comparable to the E_y component.

2.2. Measurement of the Dispersion

We have used the cavity resonator method (CRM) [11] for the measurement of the guide wavelength. The structure for the CRM measurement is shown in Fig. 2a. It consists of a dielectric core *1*, which has been bonded to the metal substrate *2*. Two identical irises *3* are connected to both ends of the IG structure. Each of the irises represents a thin metal plate *1* with a small central hole *2* (Fig. 2b).

The irises form a cavity resonator and its length in our measurement was L = 25 mm. The cavity resonator has been connected between the directional couplers for the incident and transmitted waves as is shown in Fig. 1. The power output at the swept input signal is shown in Fig. 2c.

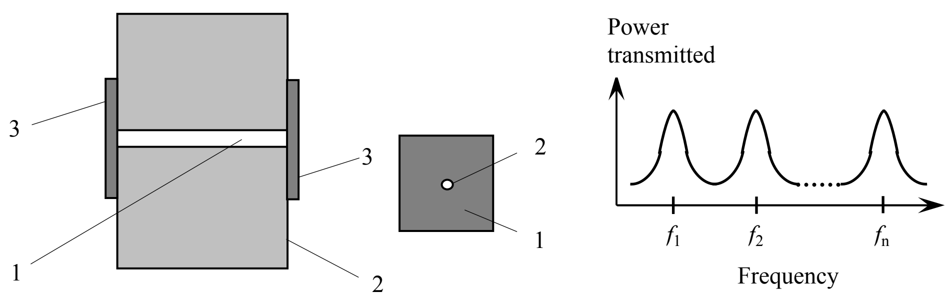

(a) (b) (c)

Fig. 2. The cavity resonator method measurement.
(a) The top view of the structure: 1 – dielectric core; 2 – metal substrate; 3 – iris.
(b) The side view (iris): 1 – thin metal plate; 2 – hole.
(c) The power output of the swept input signal

The CRM procedure is as follows. At resonance the length of the cavity L is equal to $m\lambda_g/2$, where m is an integer and the λ_g is the guide wavelength: $L = m\lambda_g/2$. Therefore, the guide wavelength is determined by the integer m. The identification of this integer could be performed by an approximate measurement of the guide wavelength with an electric probe or by a prediction of a relatively reliable theory.

2.3. Measurement of the Electric Field Components

The coaxial electric probes have been successively used earlier in the electric field sampling [5, 12]. The configuration of the structure for the electric probe measurements is shown in Fig. 3a. It consists of a dielectric core *1* bonded to the metal substrate *2* and two identical transitions with a length of 15 mm at both ends of the dielectric core. A detailed consideration about the length of the transitions could be found in [13]. The entire length of the structure was 80 mm, including both of the transitions. The transitions have been performed by a symmetrical tapering of both ends of the dielectric core *1* in an H-plane and by putting them into a Π-shaped metal body *3* (Fig. 3a). This Π-shaped body contains a groove with a cross section equal to that of the SMRW and has been connected to the metal substrate *2* with the help of the screws. The absorbing plates *4* are used in order to minimize the reflections from the Π-shaped metal body. They have a thickness of about 2.5 mm and the same Π-shaped cross section. The cross section of the IG is shown in Fig. 3b.

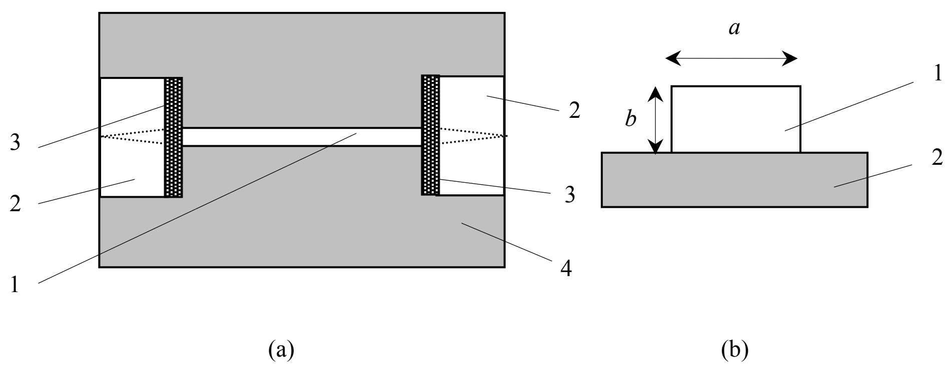

Fig. 3. The structure for the electric probe measurement.
(a) The top view of the IG structure; (b) The cross-sectional view of the IG.
1 – dielectric core; 2 – metal substrate; 3 – Π-shaped metal ; 4 – absorbing plates

The structure has been connected between the directional couplers for the incident and transmitted waves as is shown in Fig. 1a. The experimental setup permits both the loss measurement and the electric probe measurement. As far as the generator can operate both in swept and fixed frequency mode, we have had a possibility first to observe the losses in the entire frequency band, and after that to fix the desired frequency and to produce the electric field sampling with the electric probes.

The height of the electric probe above the dielectric core is correlated with the dielectric constant – the higher permittivity, the lower height. The height doesn't have to be very small in order not to disturb a lot the intrinsic field pattern. At the same time it is limited by the sensitivity of the used indicator. The height of the electric probe above the dielectric core was kept equal to 0.5 mm at all our measurements.

3. SIMULATION

We have used the 3D electromagnetic simulator HFSS (High Frequency Structure Simulator) [14] to solve numerically by the finite element method (FEM) the problem of the electromagnetic wave propagation in the alumina IG.

The geometry of the drawn model and the distribution of the electric field magnitude inside of the dielectric core for the dominant mode at a frequency of 33 GHz are shown in Fig. 4. The dimensions of the air box (20 x 10 x 10 mm^3) have to

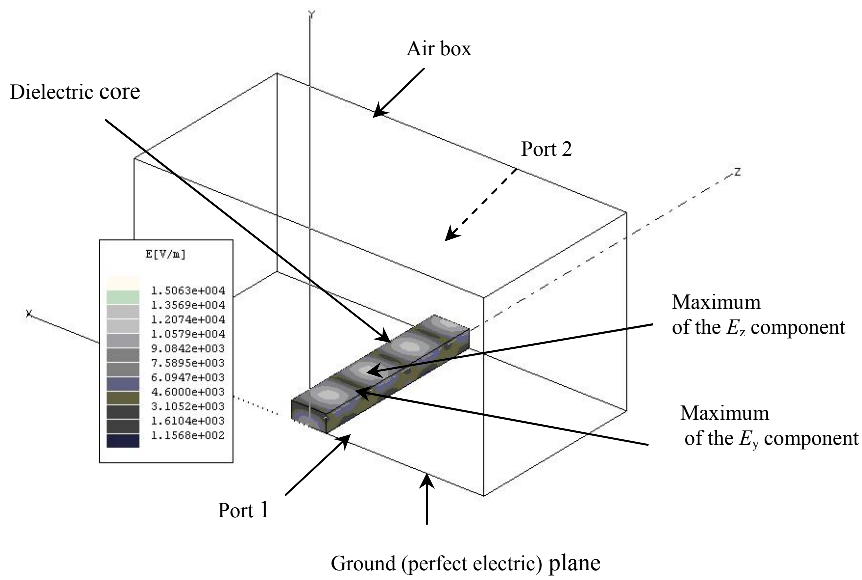

Fig. 4. The drawn model and the simulated distribution of the electric field magnitude of the dominant mode E^y_{11} inside of the dielectric core

be large enough for its upper wall and both side walls in the *yz* plane to be far enough from the correspondent walls of the dielectric core. These three walls of the air box have been defined as radiation surfaces. The bottom wall of the air box has been defined as a perfect electric (ground) plane and both side walls in the *xy* plane – as ports (Fig. 4). The lightest areas correspond to the maxima of both the electric field magnitude and the E_z component. The darkest points correspond to a maximum of the E_y component. Two adjacent light or dark places are separated by a distance of a half a guide wavelength. The guide wavelength at a frequency of 33 GHz is equal to 5.68 mm. The values of the electric field magnitude in Fig. 4 correspond to the transmitted power of 1 W.

4. RESULTS

4.1. Dispersion

The data for the guide wavelength of the dominant mode E^y_{11} in the frequency band from 28 GHz to 38 GHz are shown in Fig. 5. The simulated results obtained by the FEM have been compared with the measured data obtained by the CRM. It is evident that an excellent coincidence between simulated and measured data takes place – the relative error between the measured and the simulated guide wavelength is less than 1%. Together with the data obtained now by the FEM and CRM, the results obtained earlier [9] by the well-known effective dielectric constant method (EDCM) have been added in Fig. 5. The EDCM is an approximate method similar to the Marcatili's method that has been often used because of its relative simplicity. As it can be seen from Fig. 5 the EDCM is not quite accurate at lower frequencies – the relative error at a frequency of 37 GHz is less than 1%, but grows to about 10% at middle frequencies and to about 20% at a frequency of 29 GHz.

The simulated dispersion curves for the dominant and next two higher order modes are presented in Fig. 6. The first higher order mode appears at a frequency of 37 GHz and the second – at 42 GHz. After the examination of the field components of these higher order modes the first higher order mode has been identified as E^y_{21}, and the second – as E^x_{11} according to the Marcatili's classification. The lower frequency limit according to the dispersion definition, that is equal to the frequency at which the phase velocity of the dominant mode has changed by 20% from its value at the cutoff frequency of the first higher order mode (37 GHz), has been calculated to be equal to 33 GHz, which means that the bandwidth of a single mode operation of the IG is 4 GHz.

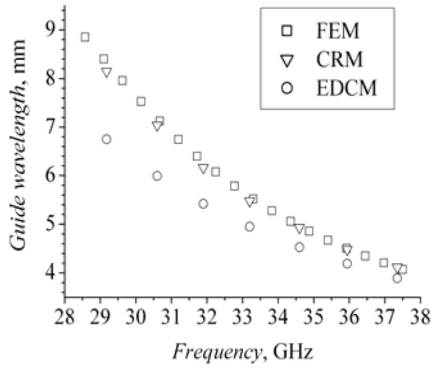

Fig. 5. Numerical and measured data for the guide wavelength of the dominant mode E^y_{11} on the alumina IG ($\varepsilon_r = 9.6$, $tg\delta_\varepsilon = 10^{-4}$; cross section of 2 x 0.97 mm^2)

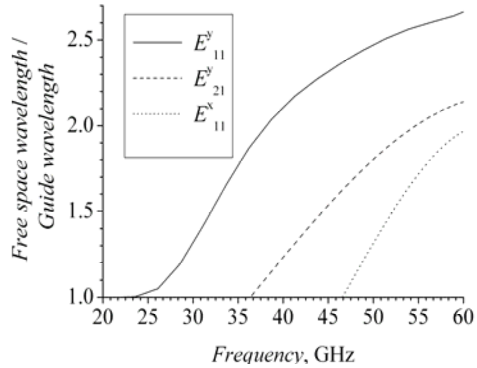

Fig. 6. Simulated dispersion curves of the first three modes on the alumina IG ($\varepsilon_r = 9.6$, $tg\delta_\varepsilon = 10^{-4}$; cross section of 2 x 0.97 mm^2)

4.2. Electric Field Components

The 3D electromagnetic simulator HFSS permits to obtain the values of all of the electric and magnetic field components at every defined point inside the model volume. After the numerical solution at a frequency of 33 GHz we have defined a number of points at two different transverse planes, $z = 0$ mm and $z = \lambda_g/4 = 1.42$ mm. The first plane corresponds to the maximum of the E_y component, and the second – to the maximum of the E_z component.

The simulated distributions at a frequency of 33 GHz for the components of the dominant mode at these planes are shown in Fig. 7 and Fig. 8. The dependence on the x coordinate has been investigated at $y = b/2 = 0.485$ mm, and the dependence on y – at $x = 0$ mm. As it can be seen from Fig. 7 and Fig. 8, the main components of the dominant mode are E_y, E_z and H_x. The comparison between the distributions in Fig. 7 and Fig. 8 shows that the E_y and E_z components have nearly equal large values at their maxima.

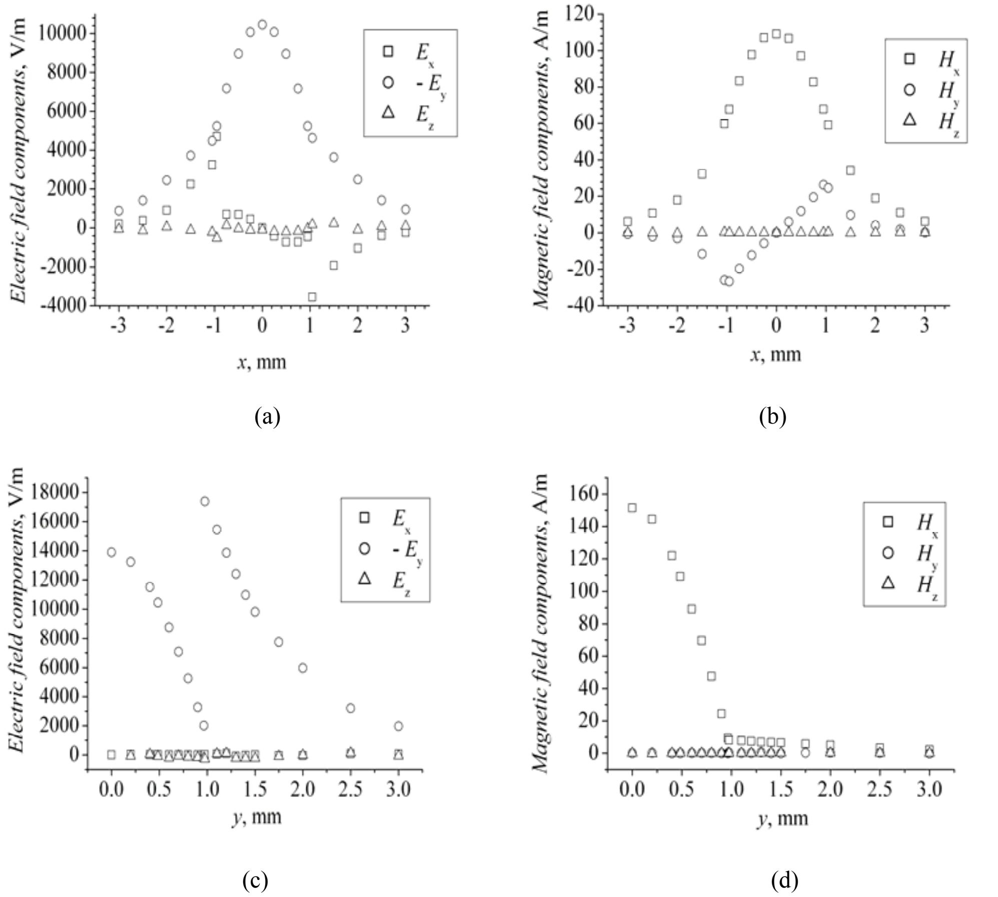

Fig. 7. Simulated distributions of the field components of the dominant mode E^y_{11} at z = 0 mm. (a, b) y = 0.485 mm; (c, d) x = 0 mm

At z = 0 mm the maxima of the E_y and H_x in the dielectric core are situated at x = 0 (Fig. 7a, b) and y = 0 (Fig. 7c, d). In accordance with the boundary conditions, the E_y component has a discontinuity at $y = b$ = 0.97 mm (Fig. 7c) as does have the E_x component at $x = \pm a/2 = \pm$ 1 mm (Fig. 7a). The H_y component has relatively small maxima at $x = \pm a/2 = \pm$ 1 mm (Fig. 7b).

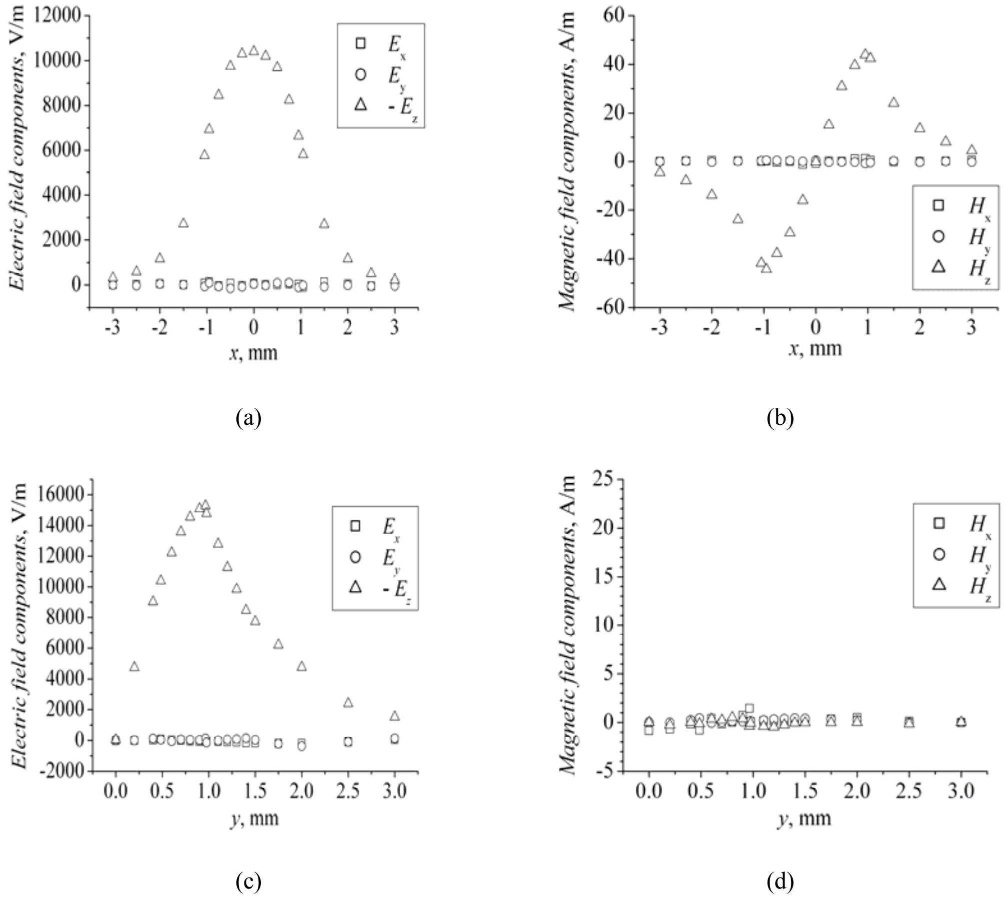

Fig. 8. Simulated distributions of the field components of the dominant mode E^y_{11} at z = 1.42 mm. (a, b) y = 0.485 mm; (c, d) x = 0 mm

At z = 1.42 mm the E_z component has a maximum at x = 0 (Fig. 8a) and $y = b$ = 0.97 mm (Fig. 8c). The greatest magnetic component at this plane is H_z, which has maxima at $x = \pm a/2 = \pm$ 1 mm (Fig. 8b). The E_x component always has a rather lesser value than the E_y component at plane z = 0 mm and than the E_z component at plane z = 1.42 mm.

In order to make some comparison with the measured distributions we have simulated the electric field at a height h above the dielectric core equal to 0.5 mm ($y - b = h$ = 0.5 mm, y = 1.47 mm) at which we have positioned the electric probe in our measurements. As it could be seen from Fig. 9, the E_x component has maxima at the planes $x = \pm a/2 = \pm 1$ mm, which are the side walls of the dielectric core. The E_y component has its maximum at $x = 0$ mm and the E_z component is practically equal to zero. The values of the components in Fig. 7 – Fig. 9 correspond to the transmitted power of 1 W.

The measured distributions at a frequency of 33 GHz are shown in Fig. 10. We have used one and the same electric probe (Fig. 1b, right) oriented along the *Ox* or *Oz* axes, and that's why we have a reason to compare the measured values. The quantity along the vertical axis, which is measured in arbitrary units, is proportional to the squared electric field components due to the square-law characteristic of the detector. The measurements have been produced at a maximum of the standing wave pattern registered by the electric probe for the principal E_y component (Fig. 1b, left).

As it could be seen from Fig. 10, the distributions are slightly asymmetrical with respect to the plane $x = 0$. There is a maximum of the measured quantity at the plane $x = 0$ when the electric probe has been oriented along the *Ox* axis. For the dominant mode the E_x component must be equal to zero at this plane because of the symmetry of the structure and is expected to have small values elsewhere, that's why the measured data represents practically the distribution of the E_y component perturbed by small levels of the E_x component. When the electric probe has been oriented along the *Oz* axis there are small maxima of the E_z component at planes $x = -2$ mm and $x = 2$ mm. As much as these planes are far enough from the dielectric core, the maxima could be treated as a result of multiple parasitic reflections in the structure from the Π-shaped metal bodies, which form the IG to SMRW transitions.

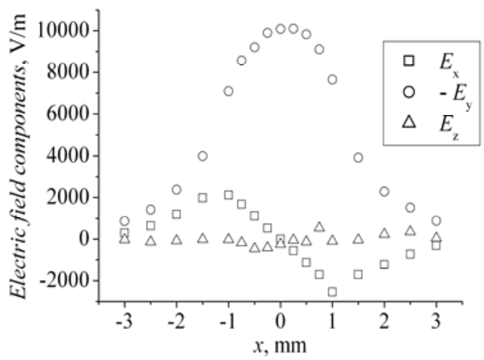

Fig. 9. Simulated distributions of the electric field components of the dominant mode E^y_{11} at $z = 0$ mm, $y = 1.47$ mm

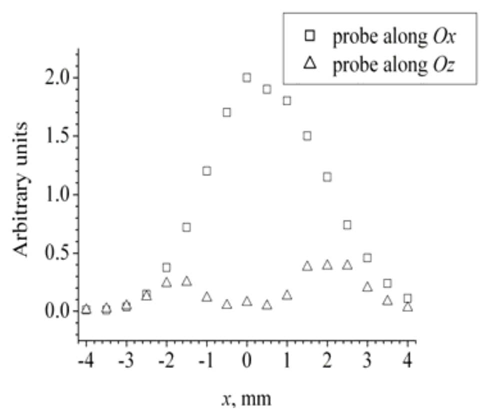

Fig. 10. Measured fields at the maximum of the standing wave pattern

5. CONCLUSION

The transverse distributions of all of the six components of the dominant mode in the alumina IG have been obtained with the help of the 3D electromagnetic simulator. A comparison between the measured and simulated results for the dispersion and the electric field components of the dominant mode has been performed. The results have shown an excellent agreement between the measured and the simulated values of the guide wavelength. The next steps of the investigation could be the simulation of the ferrite IG at different magnetizations – longitudinal, transverse and mixed one, and after that – the simulation of the coupled ferrite-dielectric IG structures with a nonreciprocal behavior.

Acknowledgements. The authors thank the Ray Sat Bg Ltd. for the possibility to use the software product Ansoft HFSS.

REFERENCES

[1] Fiedziuszko, S. J., I. C. Hunter, T. Itoh, Y. Kobayashi, T. Nishikawa, S. N. Stitzer, K. Wakino. *IEEE Trans. Microwave Theory Tech*., 2002, **50**, 706.
[2] Wolfgang Menzel. *Microwave Journal*, 2008, **51**. Available: http://www.mwjournal.com
[3] Ахумян, А. А, С.С. Гигоян, Б. А. Мурмужев, Р. М. Мартиросян. *Радиотехника*, 1990, 2, 41.
[4] Kwan, P., C. Vittoria. *IEEE Trans. Microwave Theory Tech*., 1993, **41**, 652.
[5] Arestova, I. I., S. A. Ivanov. In: *XII ICMF (International Conference on Microwave Ferrites*) *Proceedings*, 1994, 188.
[6] Marcatili, E. A. J. *Bell System Technical Journal*, 1969, **48**, 2071.
[7] Solbah, K., I. Wolff. *IEEE Trans. Microwave Theory Tech*., 1978, **26**, 266.
[8] Collier, R. J., R. D. Birch. *IEEE Trans. Microwave Theory Tech*., 1980, **28**, 932.
[9] Arestova, I. I., S. A. Ivanov. In: *XII ICMF (International Conference on Microwave Ferrites*) *Proceedings*, 1994, 183.
[10] Arestova, Iliyana I., Plamen I. Dankov, Valda P. Levcheva. In: *PIERS (Progress In Electromagnetics Research Symposium) Proceedings*, 2009, 1204.
[11] Shimabukuro, Fred I., C. Yen. *IEEE Trans. Microwave Theory Tech*., 1988, **36**, 1160.
[12] Solbach, Klaus. *IEEE Trans. Microwave Theory Tech*., 1978, **26**, 755.
[13] Arestova, Iliyana I., Valda P. Levcheva, Plamen I. Dankov. In: *TELFOR (Telecommunication forum) Proceedings*, 2009, 899.
[14] Ansoft HFSS User's Manual: A Full-Wave Spice Problem, 2001.